Desalination and Water Treatment
www.deswater.com

doi: 10.5004/dwt.2019.23423

142 (2019) 104–113
February

Investigation into the temperature effect on NOM fouling and cleaning in submerged polymeric membrane systems

Mohammad T. Alresheedi*, Onita D. Basu

Department of Civil and Environmental Engineering, Carleton University, 1125 Colonel By Drive, Ottawa, ON, K1S 5B6, Canada, Tel. +1-613-520-2600; emails: mohammadalresheedi@cmail.carleton.ca (M.T. Alresheedi), onita.basu@carleton.ca (O.D. Basu)

Received 22 July 2018; Accepted 4 November 2018

ABSTRACT

Membrane fouling is one of the main factors that hinders the wide application of ultrafiltration (UF) processes. Limited research on the influence of temperature condition on reversible and irreversible natural organic matter (NOM) fouling has been conducted. Fouling and cleaning of a submerged polymeric UF with different NOM components were examined at 5°C, 20°C, and 35°C. Fouling was evaluated using the modified fouling index-UF (MFI-UF) and unified membrane fouling index (UMFI) indices, analysis of cake layer properties, and specific flux recovery. Results showed that fouling increased by 15%–35% when water temperature decreased from 20°C to 5°C, whereas fouling decreased by 15%–25% when the temperature increased to 35°C. The $UMFI_f$ fouling order was consistent across all temperature conditions with the NOM mixture and bovine serum albumin (BSA) fouling more severely than the alginate and humic acid. The UMFI and MFI-UF exhibited the same fouling order and can be used in complement to each other. BSA was found to be more sensitive to temperature changes and irreversibly fouling more than humic acid and alginate. The ratio of irreversible to reversible fouling ($UMFI_{hir}/UMFI_{hr}$) increased by 15%–25% from 35°C to 20°C and by 30%–40% from 20°C to 5°C indicating the need for altered cleaning strategies at cold water conditions.

Keywords: Fouling indices; MFI-UF; NOM fouling; Temperature; UMFI

1. Introduction

Membrane processes are considered a reliable option for safe drinking water production. However, fouling by natural organic matter (NOM) (such as humic, protein, and polysaccharide-like substances) creates significant challenges for membrane processes to maintain good performance during operation. Fouling includes the short- and long-term loss of membrane permeability. The short-term fouling is the reversible accumulation of feedwater constituents that can be removed by hydraulic backwash and/or chemical cleaning. Long-term fouling is the long-term loss of permeability due to the irreversible accumulation of rejected materials that resist hydraulic backwash and/or chemical cleaning. Fouling is an inevitable phenomenon that results in the deterioration of membrane performance, frequent cleaning, and membrane replacements and hence increases operational cost of membrane systems.

Water temperature is a key design parameter that influences membrane operation in terms of fouling and cleaning. However, studies that have examined temperature-associated impacts with membranes are more commonly done with high-pressure systems (nanofiltration (NF) and reverse osmosis (RO)) at temperatures greater than 20°C. These types of studies tend to focus more on solution viscosity and solute diffusivity challenges with operation but not changes in fouling behavior [1,2]. Other studies have investigated temperature impacts with wastewater membrane bioreactor systems [3,4], whereas drinking water low-pressure membrane studies with a focus on lower temperatures are very limited [5,6]. In particular, the effect of low water temperatures (e.g. 5°C) have not been investigated in depth.

* Corresponding author.

Drinking water systems have in general neglected the interplay of water temperature and fouling on low-pressure membrane systems. One study [6] found that current standards for membrane integrity testing overestimated safety design values by not taking into account temperatures below 5°C highlighting the need for this type of research. Another study found that temperature affects membrane compaction and membrane resistance [7]. Very little is known on the effect of water temperature on NOM fouling and cleaning of low-pressure polymeric membranes which are critical for their design and operation for drinking water production.

Researchers have developed several methods to quantify fouling for membrane systems. Blocking laws quantify fouling location such as within the pores, pore blocking, and cake layer [8]. Fouling indices, which are considered simple and short filtration tests, are commonly used to predict the fouling potential of the membrane feed. The silt density index (SDI) and modified fouling index (MFI), using a 0.45 μm pore size membranes, have been commonly used as fouling predictors for RO membranes [9,10]. Boerlage et al. [11] developed the MFI-ultrafiltration (MFI-UF), making use of UF membranes to count for particles <0.45 μm. Feedwater having an MFI-UF <3,000 sL^{-2} is equivalent to SDI <3% min^{-1}, which is considered acceptable for membrane feed [11,12]. The utilization of the MFI-UF for assessing the fouling propensity has been carried out in recent studies with high-pressure membrane systems [13–15]. For example, Jeong et al. [13] used the MFI-UF to assess particulate and biofouling potential for RO systems. Moreover, MFI-UF was applied to assess fouling potential of different species of bloom-forming algae in marine and freshwater sources [14]. Taheri et al. [15] investigated the influence of inorganic silica and calcium colloids on the MFI-UF fouling index for seawater RO systems. The MFI-UF showed promising results with regards to assessing fouling; however, to date, the applicability of the MFI-UF testing to predict NOM fouling for low-pressure membranes has received little attention.

The unified membrane fouling index (UMFI) model [16] has been applied to quantify fouling based on hydraulic and chemical reversibility and irreversibility components. Although different fouling types, i.e. reversible versus irreversible, are well defined in the literature, inconsistent bench-scale results have been reported regarding membrane fouling by NOM, possibly due to different testing conditions, with many deviations from full-scale practice [17–19]. These studies were often conducted for short durations at conditions that do not include hydraulic backwash cycles in the testing and use of different membrane materials. Moreover, correlations between MFI-UF and UMFI for assessing NOM fouling in polymeric membrane systems under changes in water temperature condition need to be clarified.

In this research, filtration performance, NOM fouling, and chemical cleaning of a submerged polymeric UF membrane across a range of feedwater temperatures (5°C, 20°C, and 35°C) are examined. The UMFI method is utilized to assess respective reversible and irreversible fouling; while the MFI-UF is used to assess its effectiveness for predicting NOM fouling in general and under changing temperature conditions. The temperature impact on chemical cleaning is investigated with respect to membrane resistance and permeability recoveries with the various NOM solutions.

2. Materials and methods

2.1. Feed solutions

Four different synthetic feedwater solutions were used in this study to cover the range of hydrophobic and hydrophilic NOM types typically found in surface water sources [17–19]. Humic acids (2.5 mg C L^{-1}), a protein (bovine serum albumin (BSA), 2.5 mg C L^{-1}), a polysaccharide (sodium alginate, 2.5 mg C L^{-1}), and a mixture of the three NOM models (0.83 mg C L^{-1} per each NOM model, total of 2.5 mg C L^{-1}) were used as model NOM foulants. All model substances were purchased from Sigma Aldrich, Canada. A moderate hardness and alkalinity of 75 mg L^{-1} calcium carbonate ($CaCO_3$) and a low level of turbidity (5 NTU) as kaolin clay particles were included in the synthetic water matric to represent the more complex conditions of a surface water source [20].

Feed solutions were prepared using deionized water (DI) and were mixed using a magnetic stirrer 1 d prior to any experiment to ensure that materials were dissolved completely. Feedwater was continuously mixed using a VWR dual-speed mixer to ensure homogeneous water conditions throughout the experiment. The feed tank was insulated to maintain constant temperature throughout the testing period. An immersion heater (Cole Parmer, Canada) and a compact chiller (LM series, Polyscience, Canada) were used to adjust the water temperature as required. Temperature and pH were monitored continuously using HACH, Canada (cat. no. 58258-00) HQd Field Case equipment. The pH of the feed was adjusted as needed to 7.5 with NaOH. The molecular weight distribution and zeta potential of the feed solutions, which are comprised of the respective NOM components, kaolin clay, and calcium were measured using a UF fractionation method described by Kitis et al. [21] (shown in Table 1). A Malvern Zetasizer Nano was used to determine the zeta potential (ζ) of feedwater solutions. In summary, an electric field is applied via electrodes immersed in a sample, and this causes the charged particles to move toward the electrode of opposite polarity. Particle mobility is determined from the Smoluchowski model, Eq. (1) [22] (which is calculated by the Zetasizer equipment), where $\Delta E/\Delta P$ is streaming potential versus pressure; μ and k are the viscosity and the conductivity of the solution, respectively. ε_0 and ε are the permittivity of vacuum and the dielectric constant of the medium, respectively. Triplicate measurements were performed for each sample.

$$\zeta = \frac{\Delta E}{\Delta P} \times \frac{\mu k}{\varepsilon_0 \varepsilon} \tag{1}$$

2.2. Experimental setup and approach

2.2.1. Submerged polymeric membrane setup

Two submerged membrane systems were evaluated in parallel as shown in Fig. 1. Zenon ZW-1 hollow fiber (UF) membranes made of polyvinylidene fluoride, with a nominal pore size of 0.04 μm (surface area of 0.047 m^2), were used and operated under a vacuum pressure between 0 and −8.7 psi (0 and 0.6 bar). Filtration experiments were performed for 24 h under the operational conditions presented in Table 2. These

Table 1
Molecular weight fractionation and zeta potential of feed solutions

	Model feed solutions			
Molecular weight	Humic acid	BSA	Alginate	Mixture
>100 kDa	38%	51%	36%	55%
30–100 kDa	42%	44%	48%	42%
10–30 kDa	10%	2%	6%	2%
5–10 kDa	6%	1%	3%	1%
1–5 kDa	5%	2%	4%	1%
<1 kDa	2%	1%	2%	1%
Zeta potential (ζ)	–22 ± 5	–18 ± 4	–20 ± 5	–16 ± 7

operational conditions were applied based on previous work by De Souza et al. [23] and Alresheedi et al. [24]. The flow rate and direction of permeate (i.e. forward and backward) were controlled using WinLN software. Pressure readings were recorded every 10 s using Operational Flux 2.0 program.

To assess the potential seasonal impacts of water temperature on membrane fouling and cleaning, feedwater temperature was varied between 5°C, 20°C, and 35°C. Eq. (2) [22] was used to correct flux measured at different temperatures to standard temperature of 20°C. This is important as the flux greatly depends on water temperature.

$$J_{20^\circ\mathrm{C}} = J_m\left(1.03\right)^{T_{20^\circ\mathrm{C}}-T_m} \tag{2}$$

$J_{20^\circ\mathrm{C}}$ and $T_{20^\circ\mathrm{C}}$ are the flux and temperature at 20°C, respectively. J_m and T_m are the measured flux and temperature, respectively.

Table 2
Operational conditions of filtration experiments

Parameter	
Flux, LMH	38
Filtration cycle, min	15
Filtration mode	Dead-end
Backwash duration, s	20
Air scour, LPM	5
Total filtration time, h	24

Membranes were cleaned in place between each experiment following manufacturer-specified recommendations. Cleaning of the membrane units was performed in two steps: soaking in a 250 ppm of sodium hypochlorite (NaOCl) solution for 4 h followed by soaking in 1% citric acid solution for another 4 h. Chemical cleaning was conducted at room temperature. DI water was filtered through the membrane after each cleaning until a permeate flux of 38 LMH was obtained; the permeate flux was determined manually by measuring the volume produced over 1 min. Repeat cleanings were conducted until the flux 38 ± 0.50 LMH was reached.

2.2.2. Fouling resistances using the UMFI method

To assess the polymeric membrane's fouling at different water temperature conditions, the UMFI model, Eq. (3) [16], was applied to quantify each contributing fouling resistance.

$$\frac{1}{J_{s'}} = 1 + \left(\mathrm{UMFI}\right) \times V_s \tag{3}$$

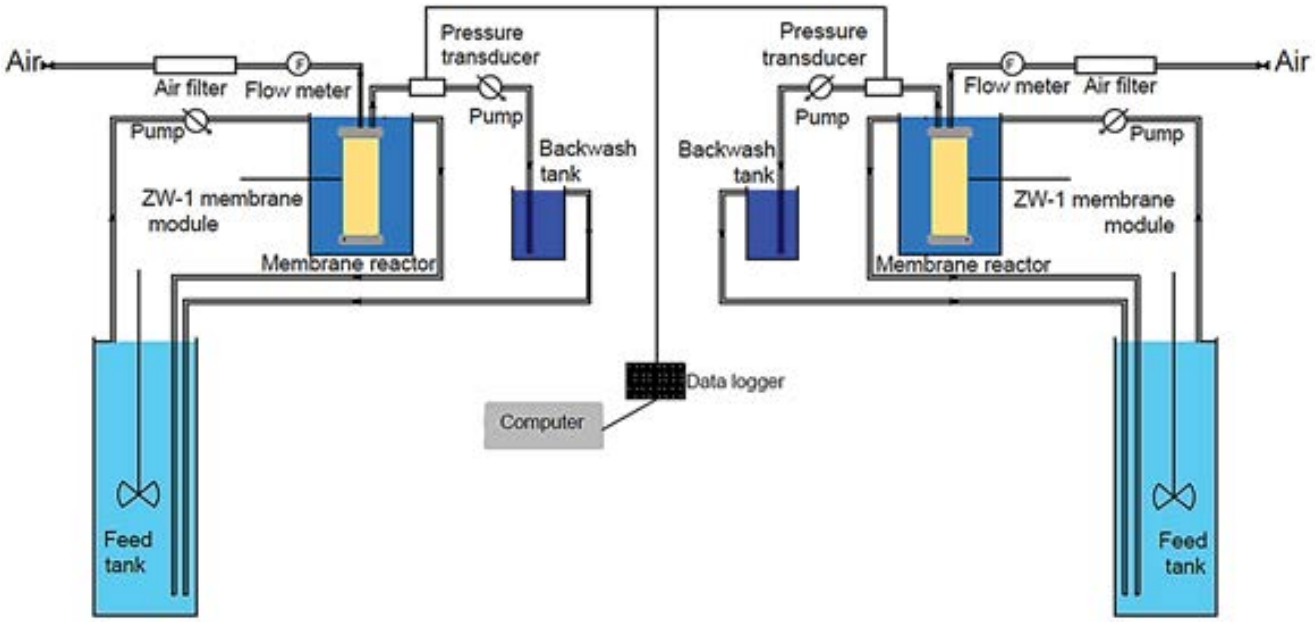

Fig. 1. A schematic representation of the bench-scale polymeric membrane setups.

where $J_{s'}$ is the normalized specific flux (unitless), UMFI is an estimate of the extent of fouling (m^{-1}), and V_s ($m^3\ m^{-2}$) is the specific permeate volume. UMFI can be calculated using Eq. (4).

$$UMFI_f = UMFI_{hr} + UMFI_{hir} = UMFI_{hr} + UMFI_{cr} + UMFI_{cir} \quad (4)$$

where $UMFI_f$ is the total fouling resistance index, $UMFI_{hr}$ is hydraulically reversible fouling resistance index (i.e. removed by backwash), and $UMFI_{hir}$ is hydraulically irreversible fouling resistance index (i.e. remained after backwash). $UMFI_{hir}$ can be divided into $UMFI_{cr}$ and $UMFI_{cir}$. $UMFI_{cr}$ is chemically reversible fouling resistance index (i.e. removable by chemical cleaning), and $UMFI_{cir}$ is chemically irreversible fouling resistance index (i.e. remained after chemical cleaning).

Fig. 2 illustrates the UMFI method used to calculate different fouling resistances. $UMFI_f$ was calculated by using filtration data from the start to end of filtration. $UMFI_{hir}$ represents the slope of the line after the start of each filtration cycle. $UMFI_{hr}$ is the difference between $UMFI_f$ and $UMFI_{hir}$. $UMFI_{cir}$ was calculated by collecting data after the chemical cleaning step. $UMFI_{cr}$ is the difference between $UMFI_{hir}$ and $UMFI_{cir}$.

2.2.3. Specific cake resistance

According to Darcy's law, the flux through a clean membrane can be written as:

$$J = \frac{\Delta P_0}{\mu R_m} \quad (5)$$

J is the membrane flux ($m^3\ m^{-2} s^{-1}$); ΔP_0 is the initial transmembrane pressure (kPa); R_m is the intrinsic membrane resistance (m^{-1}); and μ is the viscosity of the fluid (kPa s).

For fouled membrane, if all fouling is assumed to be a result of cake filtration, then Eq. (5) can be rewritten as:

$$J = \frac{\Delta P}{\mu\left(R_c + R_m\right)} \quad (6)$$

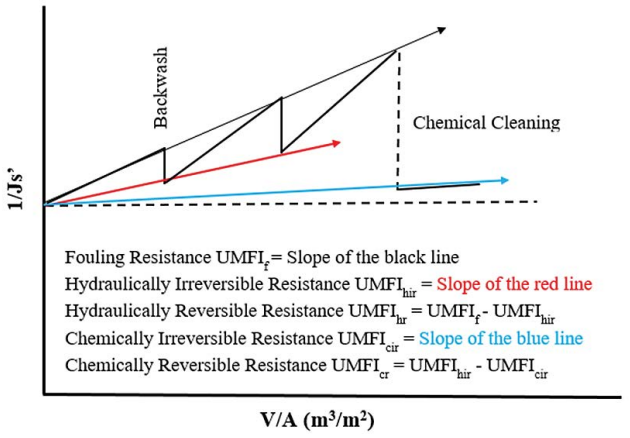

Fig. 2. Estimation of fouling resistances using the UMFI method (adapted from Alresheedi et al. [25]).

ΔP is the final transmembrane pressure (kPa); R_c is the cake layer resistance (m^{-1}).

The R_c can be expressed in terms of the specific cake resistance α_c (m kg^{-1}), the bulk concentration, C_b (kg m^{-3}), and the volume of filtered water per unit membrane area (V_s), as follows:

$$R_c = \alpha_c\, C_b\, V_s \quad (7)$$

Eqs. (5)–(7) can be combined to express the increase in transmembrane pressure at constant flux during cake filtration as shown in Eq. (8) [26].

$$\Delta P = \left(J\mu\right) \times \left(\alpha_c \times C_b \times V_s + R_m\right) = \Delta P_0 + \left(J\mu \times C_b \times V_s\right)\alpha_c \quad (8)$$

The specific cake resistance α_c often increases according to a power law [27] as shown in Eq. (9):

$$\alpha_c = \alpha_0 \times \Delta P^n \quad (9)$$

in which α_0 is a constant related primarily to the size and shape of the particles forming the cake, ΔP is final pressure, and n is the cake compressibility index, which ranges from zero (incompressible cake) to 1 or greater (for a highly compressible cake).

Scanning electron microscopy (SEM) analysis was conducted using 0.45 μm membrane filters fouled for 15 min at different feedwater temperatures. SEM images were taken at 10.00 kx magnification using the Tescan Vega-II XMU equipment for more insights into the effect of temperature on the fouling layer of different NOM fractions.

2.2.4. MFI-UF fouling index

Fouling potential of feedwater solutions from the submerged membrane experiments (i.e. humic acids, BSA, alginate, and NOM mixture) was assessed using the MFI-UF method [11]. Fouling indices are used to measure and predict the fouling potential of membrane feedwater, diagnose fouling at the design stage, and/or monitor pretreatment performance during membrane operation. The MFI-UF setup is described in detail by Boerlage et al. [11]. The characteristics of the MFI-UF membrane are presented in Table 3.

Table 3
MFI-UF membrane characteristics

	MFI-UF membrane
Membrane type	UF – 13 kDa
Membrane materials	PAN hollow fiber (Pall Corp., Canada)
Configuration	Inside out
Fiber inside diameter, mm	0.8
Fiber outside diameter, mm	1.4
Number of fibers	400
Membrane area, m^2	0.2
Module length, mm	347
Module diameter, mm	42

MFI-UF testing was determined according to the method described by Boerlage et al. [11]. Feedwater was filtered through the hollow fiber UF membrane under dead-end mode and pressure of 2 bar. Permeate was collected in a tank set on the electronic balance to acquire permeate volume (V) and filtration time (t) data from the balance. The MFI-UF_{exp} was then calculated using Eq. (10) [10]. $d(t/V)/dV$ is the slope of two data points in the linear region of t/V vs. V graph (described in detail by Boerlage et al. [11]).

$$\text{MFI} - \text{UF}_{\text{exp}} = \frac{d\left(\frac{t}{V}\right)}{dV} \tag{10}$$

The MFI-UF test was performed under the same water temperature conditions as the submerged polymeric membrane experiments (i.e. 5°C, 20°C, and 35°C).

3. Results and Discussion

3.1. Effect of water temperature condition on NOM fouling

Fig. 3(a)–(d) shows the inverse of the normalized specific flux ($1/J_s$) versus filtered water volume per membrane area (V/A). It can be clearly seen that the changes in NOM fouling with temperature are over and beyond simple viscosity changes in water. Water temperature was found to impact NOM fouling as follows: an increase in water temperature resulted in lower fouling rate for all NOM solutions. Overall, as temperature decreased from 20°C to 5°C, membrane fouling increased by 15%–35%, whereas fouling decreased by 15%–25% when the temperature increased from 20°C to 35°C. The changes in NOM fouling behavior with temperature could be attributed to the changes in the membrane structure and properties such as porosity and resistance which may impacted the fouling layer formed and NOM retention [28]. Thus, changes in water temperature condition could be crucial factor for membrane systems to meet consistent performance targets.

Fig. 3 also shows that different NOM fractions responded differently to temperature changes. BSA is more sensitive to temperature changes in which fouling was observed to increase by 35% with decreasing temperature from 20°C to 5°C compared with 15% and 20% for humic acid and alginate, respectively. In addition, fouling of the NOM mixture is approximately similar to BSA alone, indicating a higher effect from protein substances on fouling. The differences between fouling among the types of NOM could be partially attributed to the molecular weight distribution and zeta potential (as shown in Table 1). For humic acid and sodium alginate feedwater solutions, there were larger components with molecular weight in the range of 30–100 kDa, which were smaller than the pore size of the membrane (0.04 μm) and may therefore adsorbed on the pore surface and cause internal fouling or passed through the membrane to the permeate side. On the other hand, BSA and NOM mixture feedwater solutions had a larger fraction of components with molecular weight >100 kDa, which may have caused pore blocking during the early stages of filtration and/or adsorbed on the pore surface leading to higher fouling compared with humic acid and sodium alginate.

Moreover, the zeta potential values of BSA and NOM mixture feedwater (–18 and –16 mV, respectively) were lower than that for humic acid and alginate feedwater (–22 and –20 mV, respectively) and would have a higher tendency to adsorb on the membrane surface or pores. Similar results were reported by the study of Contreras et al. [29] in which BSA had a lower zeta potential (–20.7 mV) compared with sodium alginate (–45.0 mV) and humic acid (–37.9) leading to lower electrostatic repulsion and higher hydrophobic interaction between BSA and thin-film composite NF membrane. Interestingly, sodium alginate (hydrophilic) resulted in higher fouling compared with humic acid (hydrophobic) indicating a strong influence from polysaccharides on membrane fouling compared to humic substances. These results are consistent with those reported by Hashino et al. [19] in which the sodium alginate solution showed more severe flux decline than humic acid with MF membranes.

Additionally, the specific cake resistance (α_c) and compressibility index (n) were calculated from the experimentally determined values of the filtration pressure, bulk concentration, and specific filtered water volume, considering cake filtration is the dominant fouling mechanism [30], as described in Eqs. (5)–(9). Fig. 4(a) shows that α_c value of all NOM models decreases as feedwater temperature increases from 5°C to 35°C; therefore, temperature influences the NOM cake structure. Jin et al. [1] found that humic acid colloids decreased in size with increasing temperature of RO feed. As a result, smaller particles produced more porous deposits and influenced fouling. In this study, the decrease in α_c with increasing temperature could be attributed to the decrease in NOM size which may have changed the cake layers into more porous and open structures. Thus, lower fouling was obtained at higher temperature. Furthermore, Fig. 4(a) and (b) shows that BSA and NOM mixture cake resistances are significantly affected by temperature; changes in cake resistance with temperature indicate more compressible cake (n = 0.85 and 0.89 for BSA and NOM mixture, respectively). This is reflected in Fig. 3, where the fouling trend for BSA and NOM mixture changes significantly, particularly between 5°C and 20°C. The compressibility indices for humic acid and sodium alginate are quite similar (0.57 and 0.59, respectively), which differ from those of Sioutopoulos et al. [31] who found that humic acid deposits are more compressible (n = 0.70) compared with alginate deposits (n = 0.40) with UF membranes. The difference in the actual numerical value of n may be caused by the different membrane material and/or the high concentration of total dissolved solids in the solutions used by Sioutopoulos et al. [31].

To visualize the effect of temperature on NOM fouling layer properties, Fig. 5 shows SEM images of humic acid, BSA, and sodium alginate fouling layers. The SEM analyses were conducted using 0.45 μm membrane filters fouled for 15 min at constant pressure of 1 bar and different feedwater temperatures. From Fig. 5, it can be clearly seen that the fouling layer differs between different NOM components. At 20°C, humic acid filled the pores partially and developed a layer of open structure, whereas protein and sodium alginate developed a rough gel layer and appeared to fill more pores compared to humic acid. This is reflected in Fig. 3, where the fouling for BSA and alginate was higher than humic acid. Fig. 5 also shows a decrease in water temperature from 20°C to 5°C

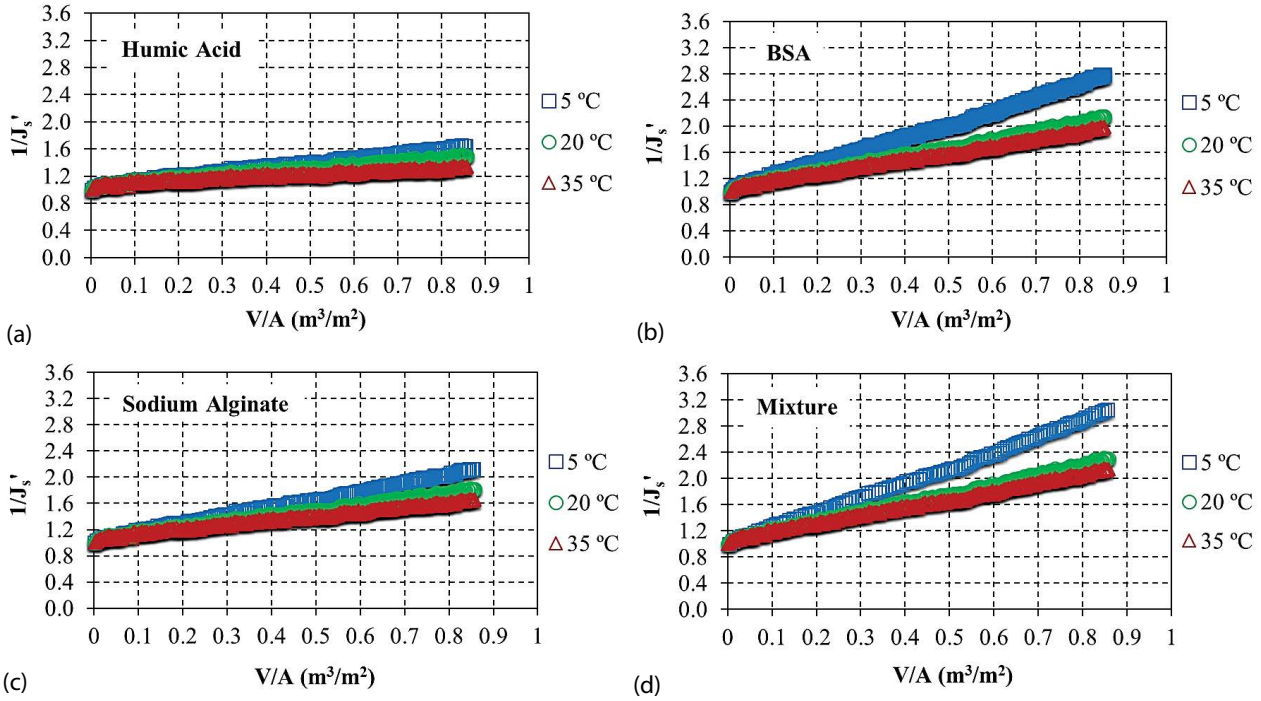

Fig. 3. NOM fouling graphs (a) humic acid; (b) BSA; (c) sodium alginate; (d) mixture. *Js'*: normalized specific flux; *V/A*: filtered water volume per membrane area.

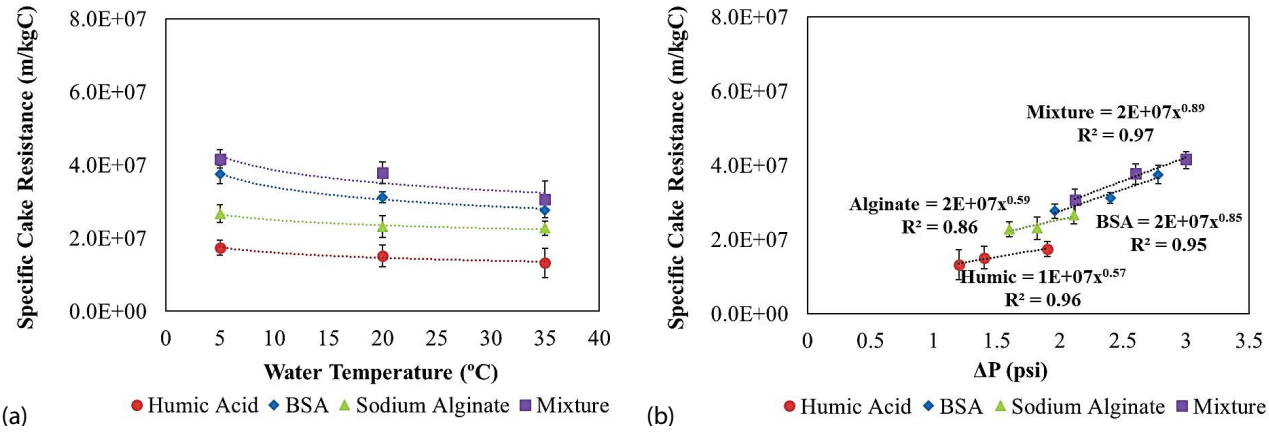

Fig. 4. (a) Changes in specific cake resistance with temperature; (b) estimated compressibility index values.

resulting in more compact layer for all NOM components. More specifically, at 5°C, BSA completely blocked membrane pores and developed a fouling layer of high resistance. This can be supported by the findings from Fig. 4, in which BSA has the highest specific fouling resistance and compressibility index values compared to alginate and humic acid.

3.2. Fouling indices assessment at different water temperature conditions

3.2.1. Reversible and irreversible fouling indices

To quantify membrane fouling during membrane filtration, fouling resistances using the UMFI were estimated. The lower the $UMFI_{hir}/UMFI_{hr}$ ratio the more effective the hydraulic backwashes, due to greater cake formation, while the higher the $UMFI_{hir}/UMFI_{hr}$ ratio the greater the NOM adsorption and pore blockage and thus a greater need for chemical cleans as hydraulic backwashes are less effective. The hydraulically irreversible fouling index ($UMFI_{hir}$) can be categorized into the chemically reversible fouling ($UMFI_{cr}$) and the chemically irreversible fouling ($UMFI_{cir}$). $UMFI_{cr}/UMFI_{hir}$ quantifies the irreversible fouling ratio removed by a chemical clean while $UMFI_{cir}/UMFI_{hir}$ quantifies the fouling ratio that remains after a chemical clean. Minimizing chemical cleans is preferred to help control membrane aging which decreases the hydraulic resistance and hydrophobicity of membrane material [32]. Moreover, controlling the degree of

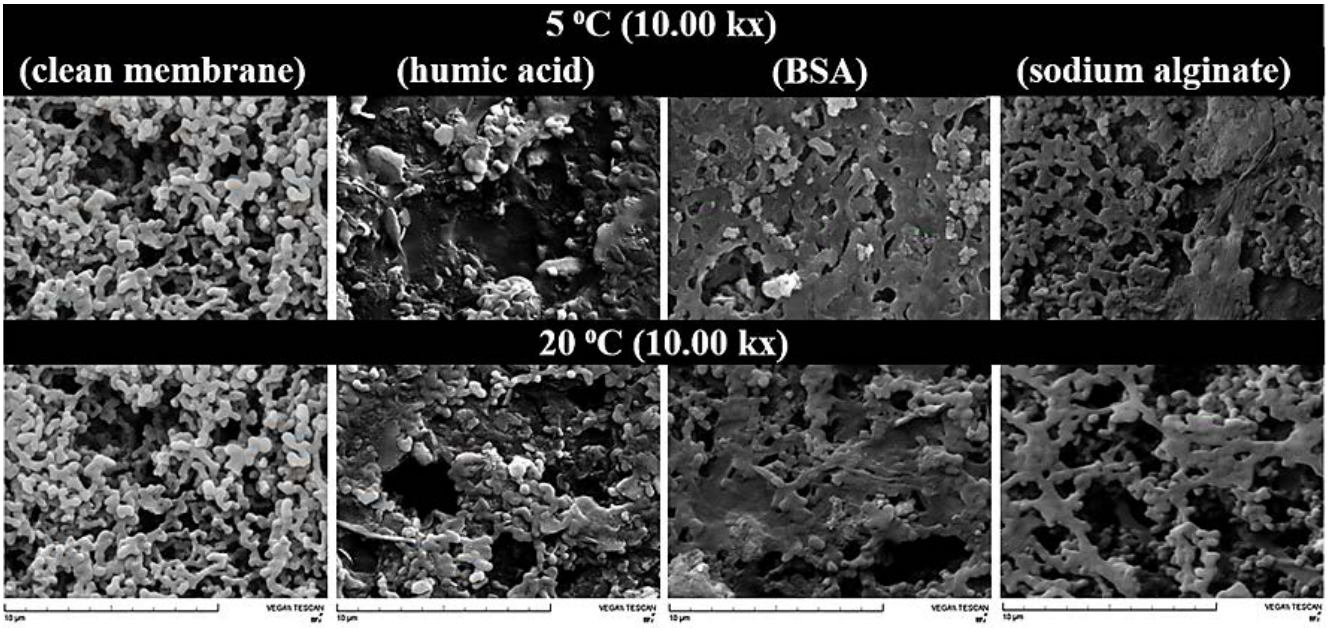

Fig. 5. SEM images of NOM fouling layers at 5°C and 20°C (P = 1 bar) using 0.45 μm membrane filters.

chemical cleaning helps minimize chemical waste production and maintain membrane productivity. Fig. 6(a)–(c) shows the UMFI values estimated at different tested water temperature conditions. The $UMFI_f$ fouling index order was consistent at different temperatures, which was the highest for the NOM mixture followed by BSA, alginate, and lastly humic acid. The similar $UMFI_f$ values for the NOM mixture and the BSA solution indicate that protein-based NOM significantly contributes to fouling in membrane systems. Hashino et al. [19] similarly reported a significant flux decline of cellulose acetate butyrate membrane caused by BSA adsorption compared with alginate. Moreover, BSA fouling (Fig. 6) is more sensitive to changes in water temperature condition in which BSA $UMFI_f$ increased by 35% with decreasing temperature from 20°C to 5°C compared with 15% and 20% for humic acid and alginate, respectively.

To quantify the effect of water temperature on NOM fouling behaviors, Fig. 7 presents the changes in irreversible to reversible fouling index ratios ($UMFI_{hir}/UMFI_{hr}$) under all tested water temperature conditions. The $UMFI_{hir}/UMFI_{hr}$ ratios of all NOM models were the highest during the 5°C operation (1.8–3.3), compared with 20°C (0.95–1.9) and 35°C (0.7–1.3). The increase in the $UMFI_{hir}/UMFI_{hr}$ at lower temperature indicates lower hydraulic backwash efficiency, thus higher NOM irreversibility. This can be supported by the increase in specific cake resistance observed in Fig. 4(a). The $UMFI_{hir}/UMFI_{hr}$ ratios decreased by about 30%–40% as feedwater temperature increased from 5°C to 20°C and by about 15%–25% as the temperature increased from 20°C to 35°C. Therefore, hydraulic backwashing at warm water temperature (i.e. 20°C and 35°C) was more effective in removing the hydraulically irreversible fouling of NOM compared with cold water temperature, 5°C. Irreversibility of the foulant layer is a major concern during membrane filtration, as it influences the requirement to initiate hydraulic or chemical cleaning actions. Although hydraulic backwashing was efficient in mitigating a large percentage of NOM fouling at warm water temperature condition, the significant amount of irreversible fouling due to stronger adsorption of foulants actually poses a potential limitation to longer membrane operation.

3.2.2. Correlation of UMFI and MFI-UF indices

The MFI-UF method is used to assess the fouling tendency of a membrane feed, whereas the UMFI provides information on the current fouling a membrane is subjected to. Thus, the MFI-UF is used to predict fouling while the UMFI is used to quantify fouling in an operating system. Feedwater having an MFI-UF <3,000 s L^{-2} (equivalent to an SDI < 3% min^{-1}) is considered acceptable for membrane feed [11]. However, the actual capacity of the MFI-UF to be used effectively as a prediction tool with NOM has yet to be evaluated in general and under changing water temperature conditions. Table 4 presents fouling index values predicted by the MFI-UF method. The results in Table 4 show an increased fouling potential across all NOM sources as the water temperature drops, which is in agreement with the increased fouling tendency observed in Fig. 7 using the UMFI method. The NOM fouling potential predicted by the MFI-UF was in the order of mixture > BSA > sodium alginate > humic acid, which matches the fouling trend observed in the submerged polymeric UF system with the UMFI method.

Fig. 8 compares fouling resistances estimated by the UMFI method to the MFI-UF for various NOM foulants at different temperature conditions. From Fig. 8, it can be observed that the MFI-UF values correlate well with the $UMFI_f$ (R^2 = 0.76) and $UMFI_{hir}$ (R^2 = 0.86). Since fouling irreversibility poses major implications during filtration with respect to membrane cleaning and life time, the MFI-UF testing method demonstrates a useful fit for predicting fouling before relying on operating data. Thus, a plant could use the MFI-UF

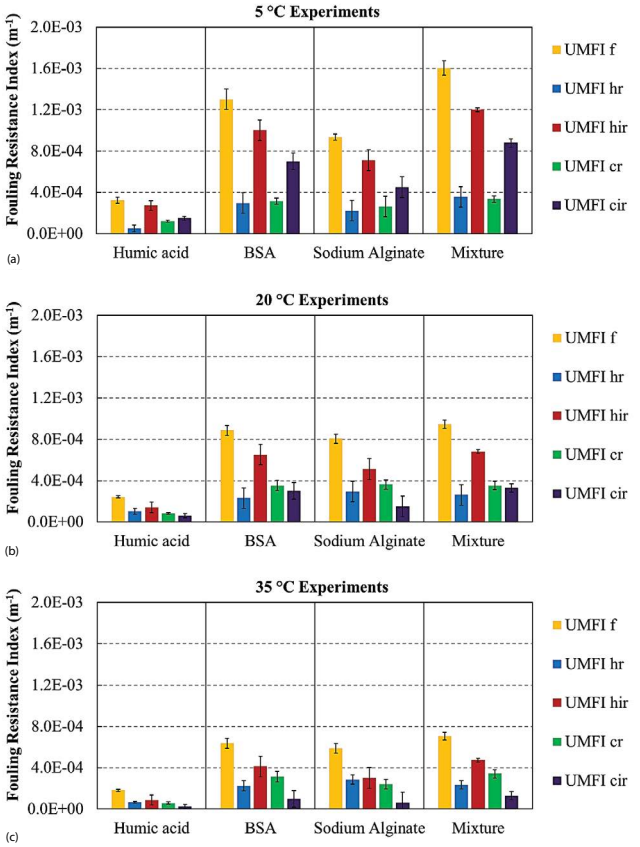

Fig. 6. Estimated UMFI values at different temperature conditions. Note: $UMFI_f$: unified total fouling index; $UMFI_{hr}$: unified hydraulically reversible fouling index; $UMFI_{hir}$: unified hydraulically irreversible fouling index; $UMFI_{cr}$: unified chemically reversible fouling index; $UMFI_{cir}$: unified chemically irreversible fouling index.

to monitor and predict changes in irreversible fouling with temperature and make required alternations in membrane pretreatment and/or cleaning procedures.

3.3. Impact of water temperature on chemical cleaning

As noted above, fouling with NOM across all model solutions increased as the water temperature decreased; additional tests were conducted to assess for changes in cleaning effectiveness with temperature as well. Fig. 9 shows

Table 4
MFI-UF index prediction of NOM fouling at different temperatures

	Humic acid	BSA	Sodium alginate	Mixture
		MFI-UF (s L^{-2})		
5°C	5,559 ± 294	9,880 ± 332	6,948 ± 186	10,122 ± 491
20°C	3,487 ± 300	6,200 ± 220	5,018 ± 222	6,850 ± 495
35°C	1,350 ± 45	3,511 ± 353	2,144 ± 62	3,774 ± 152

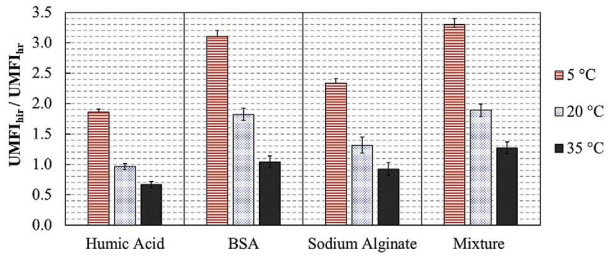

Fig. 7. Hydraulically irreversible to reversible fouling index ratios at different water temperature conditions. Note: $UMFI_{hir}$/$UMFI_{hr}$ ratio of 1 indicates 50% irreversible and 50% reversible fouling. Ratio > 1 indicates higher irreversible fouling.

the ratio of chemically reversible fouling to hydraulically irreversible fouling indices, $UMFI_{cr}$/$UMFI_{hir}$ (Fig. 9(a)), and specific flux recoveries (Fig. 9(b)) at different water temperatures. From Fig. 9(a), it can be clearly seen that the $UMFI_{cr}$/$UMFI_{hir}$ ratios differ at different water temperatures. Under the operation at 5°C, chemical cleaning efficiency was the lowest and increased by 10%–40% ($p < 0.05$), with increasing filtration temperature from 5°C to 20°C. Thus, the initial chemical cleaning protocol recommended by the polymeric membrane manufacturer (i.e. NaOCl followed by citric acid) was not sufficient in removing irreversible fouling at 5°C compared with 20°C. The decrease in the cleaning efficiency with temperature is attributed to the high irreversible fouling ratio at 5°C as observed in Fig. 7. Moreover, as water temperature increased from 20°C to 35°C, the $UMFI_{cr}$/$UMFI_{hir}$ ratios also increased but moderately by 10%–15% ($p < 0.05$). The $UMFI_{cr}$/$UMFI_{hir}$ ratios of the NOM mixture and BSA were always lower than that for alginate and humic acids, indicating lower cleaning efficiency for the NOM mixture and BSA. This attributes to the higher irreversible fouling observed with the NOM mixture and BSA compared with the alginate and humic acid waters. Clearly, a more aggressive chemical cleaning strategy is required to better remove NOM mixture and BSA fouling at the lower temperature, highlighting the need to focus on both NOM type and water temperature to optimize chemical cleaning regimes.

The influence of filtration temperature on NOM chemical cleaning can also be observed in Fig. 9(b). The specific flux recoveries at 5°C, after one cleaning cycle using NaOCl followed by citric acid, ranged from 85% to 95%, which were

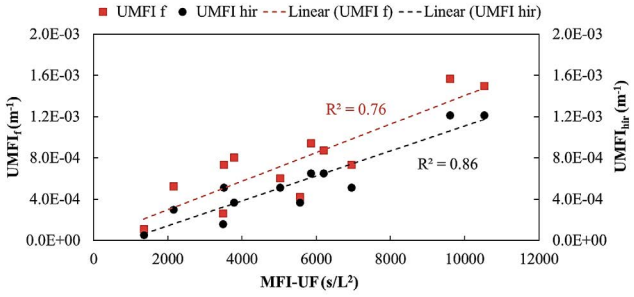

Fig. 8. Relationship between UMFI fouling resistances and MFI-UF fouling index.

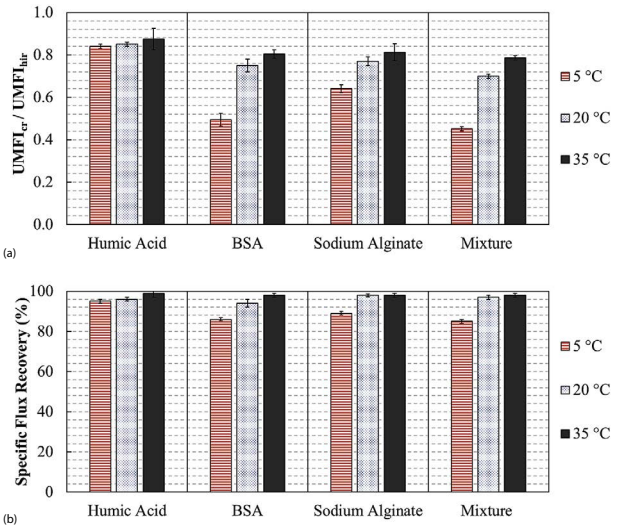

Fig. 9. Chemical cleaning efficiency at different filtration water temperatures: after one cleaning cycle using NaOCl followed by citric acid. (a) $UMFI_{cr}/UMFI_{hir}$ ratios: the higher the $UMFI_{cr}/UMFI_{hir}$ ratio the higher the chemical cleaning efficiency; (b) Specific flux recovery.

significantly lower ($p < 0.05$) than those obtained at 20°C (ranged from 95% to 98%). The difference in the specific flux recovery at 5ºC and 20ºC conditions is attributed to the differences in the irreversible fouling ratios as shown in Fig. 7. Thus, a more aggressive cleaning was needed to recover specific flux at 5°C compared with 20°C. This can be supported by the specific flux recovery values at 35°C in which all NOM types were effectively removed, and the specific flux recovery was >95%. In addition, at 5°C, the NOM mixture, BSA, and alginate required an additional 1 h cleaning using NaOCl (i.e. after the one recommended cleaning cycle using NaOCl followed by citric acid) to achieve >95% of specific flux recovery (results not shown). On the other hand, at 20°C and 35°C, membranes were able to achieve >95% after only one cleaning cycle. Humic acid cleaning was less affected by temperature variation compared with the other NOM models (refer to Fig. 9(a) and (b)). These results indicate the need to emphasize good pretreatment or modification of cleaning steps by applying higher backwash pressure and/or higher chemical concentrations during membrane operation in cold climates to mitigate NOM fouling and ensure higher specific flux recovery.

4. Conclusions

Limited research has investigated changes in NOM fouling and cleaning with temperature with polymeric UF membranes. This research investigated the impact of water temperature at 5°C, 20°C, and 35°C on NOM fouling and cleaning using the UMFI and MFI-UF methods with the following key observations:

- Feedwater temperature has a significant impact on submerged polymeric UF membrane fouling. Fouling increased by 15%–35% when the water temperature decreased from 20°C to 5°C while the fouling decreased by 15%–25% when the temperature increased to 35°C. Thus, fouling analysis for plant subject to cold water conditions should be investigated more rigorously to help maintain membrane productivity.
- BSA was more sensitive to changes in water temperature, whereas humic acid was less sensitive, highlighting the need to identify specific NOM fractions in water to better understand potential fouling changes.
- The MFI-UF fouling prediction trend was in strong agreement with UMFI indices for establishing NOM irreversible fouling, highlighting an advantage of the MFI-UF as a robust fouling prediction index for low-pressure polymeric membranes.
- Aside from humic acid, chemical cleaning of all other NOM solutions was less efficient at the colder water temperature and thus indicates the need for alternative chemical cleaning strategies during lower water temperature conditions to recover membrane permeability.

Acknowledgements

The authors would like to acknowledge the Saudi Arabia Ministry of Education (MOE) and Natural Sciences and Engineering Research Council of Canada (NSERC) for helping fund this research. The authors would also like to thank summer student, Bia Pereira, for her hard work and help in the laboratory.

References

[1] X. Jin, A. Jawor, S. Kim, E.M.V. Hoek, Effects of feed water temperature on separation performance and organic fouling of brackish water RO membranes, Desalination, 239 (2009) 346–359.
[2] Y. Roy, D. Warsinger, J. Leinhard, Effect of temperature on ion transport in nanofiltration membranes: diffusion, convection and electro migration, Desalination, 420 (2017) 241–257.
[3] J. Arevalo, L. Ruiz, J. Perez, M. Gomez, Effect of temperature on membrane bioreactor performance working with high hydraulic and sludge retention time, Biochem. Eng. J., 88 (2014) 42–49.
[4] Z. Ma, X. Wen, F. Zhao, Y. Xia, X. Huang, D. Wait, J. Guan, Effect of temperature variation on membrane fouling and microbial community structure in membrane bioreactor. Bioresour. Technol., 133 (2013) 462–468.
[5] T. Steinhauer, S. Hanely, K. Bogendörfer, U. Kulozik, Temperature dependent membrane fouling during filtration of whey and whey proteins, J. Membr. Sci., 492 (2015) 364–370.
[6] K. Farahbakhsh, D. Smith, Membrane filtration for cold regions – impact of cold water on membrane integrity testing, J. Environ. Eng. Sci., 5 (2006) 69–75.
[7] S. Stade, M. Kallioinen, T. Tuuva, M. Manttari, Compaction and its effect on retention of ultrafiltration membranes at different temperatures, Sep. Purif. Technol., 151 (2015) 211–217.
[8] J. Hermia, Constant pressure blocking filtration laws application to power-law non-newtonian fluids, Trans. Inst. Chem. Eng., 60 (1982) 183–187.
[9] ASTM International, Standard test method for silt density index (SDI) of water, Designation: D4189–07 (Reapproved 2014).
[10] J. Schippers, J. Verdouw, The modified fouling index, a method of determining the fouling characteristics of water, Desalination, 32 (1980) 137–148.
[11] S. Boerlage, M. Kennedy, M. Dickson, D. El-Hodali, J. Schippers, The modified fouling index using ultrafiltration membranes (MFI-UF): characterisation, filtration mechanisms and proposed reference membrane, J. Membr. Sci., 197 (2002) 1–21.

[12] S. Boerlage, M. Kennedy, M. Aniye, E. Abogrean, Z. Tarawneh, J. Schippers, The MFI-UF as a water quality test and monitor, J. Membr. Sci., 211 (2003) 271–289.
[13] S. Jeong, S. Vigneswaran, Practical use of standard pore blocking index as an indicator of biofouling potential in seawater desalination, Desalination, 365 (2015) 8–14.
[14] L. Villacorte, Y. Ekowati, H. Winters, G. Amy, J. Schippers, M. Kennedy, MF/UF rejection and fouling potential of algal organic matter from bloom-forming marine and freshwater algae, Desalination, 367 (2015) 1–10.
[15] A. Taheri, L. Sim, C. Haur, E. Alkhondi, A. Fane, The fouling potential of colloidal silica and humic acid and their mixtures, J. Membr. Sci., 433 (2013) 112–120.
[16] H. Huang, T. Young, J. Jacangelo, Unified membrane fouling index for low pressure membrane filtration of natural waters: principles and methodology, Environ. Sci. Technol., 42 (2008) 714–720.
[17] H. Chang, H. Liang, F. Qu, S. Shao, H. Yu, B. Liu, W. Gao, G. Li, Role of backwash water composition in alleviating ultrafiltration membrane fouling by sodium alginate and the effectiveness of salt backwashing, J. Membr. Sci., 499 (2016) 429–441.
[18] K. Katsoufidou, D. Sioutopoulos, S. Yiantsios, A. Karabelas, UF membrane fouling by mixtures of humic acids and sodium alginate: fouling mechanisms and reversibility, Desalination, 264 (2010) 220–227.
[19] M. Hashino, K. Hirami, M. Katagiri, T. Kubota, Effects of three natural organic matter types on cellulose acetate butyrate microfiltration membrane fouling, J. Membr. Sci., 379 (2011) 233–238.
[20] D. Jermann, W. Pronk, M. Boller, Mutual influences between natural organic matter and inorganic particles and their combined effect on ultrafiltration membrane fouling, Environ. Sci. Technol., 42 (2008) 9129–9136.
[21] M. Kitis, T. Karanfil, A. Wigton, J. Kilduff, Probing reactivity of dissolved organic matter for disinfection by products formation using XAD-8 resin adsorption and UF fractionation, Water Res., 36 (2002) 3834–3848.
[22] J. Crittenden, R. Trussell, D. Hand, K. Howe, G. Tchobanoglous, Water Treatment: Principles and Design, 2nd edition, Wiley, New Jersey, USA, 2005.
[23] N. De Souza, O. Basu, Comparative analysis of physical cleaning operations for fouling control of hollow fiber membranes in drinking water treatment, J. Membr. Sci., 436 (2013) 28–35.
[24] M. Alresheedi, O. Basu, Support media impacts on humic acid, cellulose, and kaolin clay in reducing fouling in a submerged hollow fiber membrane system, J. Membr. Sci., 450 (2014) 282–290.
[25] M. Alresheedi, O. Basu, Fouling indices and resistance in series methods for quantification of NOM fouling in submerged polymeric membrane systems, IWA Membrane Technology Conference, Singapore, 2017.
[26] S. Chellam, X. Wendong, Blocking laws analysis of dead-end constant flux microfiltration of compressible cakes, J. Colloid Interface Sci., 301 (2006) 248–257.
[27] G. Foley, A review of factors affecting filter cake properties in dead-end microfiltration of microbial suspensions, J. Membr. Sci., 274 (2006) 38–46.
[28] L. Cui, C. Goodwin, W. Gao, B. Liao, Effect of cold water temperature on membrane structure and properties, J. Membr. Sci., 540 (2017) 19–26.
[29] A. Contreras, A. Kim, Q. Li, Combined fouling of nanofiltration membranes: mechanisms and effect of organic matter, J. Membr. Sci., 327 (2009) 87–95.
[30] M. Alresheedi, O. Basu, Application of MFI-UF fouling index with NOM fouling under various operating conditions, Desal. Wat. Treat., 133 (2018) 45–54.
[31] D. Sioutopoulos, S. Yiantsios, A. Karabelas, Relation between fouling characteristics of RO and UF membranes in experiments with colloidal organic and inorganic species, J. Membr. Sci., 350 (2010) 62–82.
[32] Q. Wang, H. Zeng, Z. Wua, J. Cao, Impact of sodium hypochlorite cleaning on the surface properties and performance of PVDF membranes, Appl. Surf. Sci., 428 (2018) 289–295.